Dalton Transactions

PERSPECTIVE

View Article Online
View Journal | View Issue

Cite this: *Dalton Trans.*, 2015, **44**, 8771

Received 6th February 2015,
Accepted 17th March 2015

DOI: 10.1039/c5dt00549c

www.rsc.org/dalton

Heterometallic 3d–4f single-molecule magnets

Lidia Rosado Piquer and E. Carolina Sañudo*

The promising potential applications, such as information processing and storage or molecular spintronics, of single-molecule magnets (SMMs) have spurred on the research of new, better SMMs. In this context, lanthanide ions have been seen as ideal candidates for new heterometallic transition metal–lanthanide SMMs. This perspective reviews 3d–4f SMMs up to 2014 and highlights the most significant advances and challenges of the field.

Introduction

In the early 1990s the discovery that transition metal complexes could retain magnetization caused an explosion in the field of coordination complexes. The first molecule that was shown to act as a magnet at the molecular level was a dodecanuclear complex of Mn(III)/Mn(IV) with acetato, oxo and water ligands, $[Mn_{12}O_{12}(MeCOO)_{16}(H_2O)_4]$, $Mn_{12}Ac$.[1] Molecules with this property were then called single-molecule magnets (SMMs). Soon other transition metal complexes were also found to be SMMs, including a large family of Mn_{12} complexes with structures related to that of $Mn_{12}Ac$. $Mn_{12}Ac$ was the first SMM discovered and is still one of the most studied. SMMs are by themselves already very interesting molecules with very special magnetic properties, but their discovery also brought about the possibility of their use in technological applications, substituting conventional ferromagnetic materials for SMMs. The promise of the use of SMMs in the processing and storage of information is not only that of the use of a new material for the same task, but that of opening up the possibility of having ultra-high density information storage devices, or ultra-fast information processing devices based on SMMs. Additionally, as new SMMs are discovered, new applications are proposed, for example their use in molecular spintronics. There are two main problems that must be solved before all these proposed technological applications of SMMs can be implemented. Firstly, the working temperatures must be improved, so far all SMMs discovered to date only function at liquid helium temperatures. This in itself does not make them useless, but it greatly holds them back from any applications in information storage and processing, which is nowadays efficiently done with bulk ferromagnetic materials, or even spintronics. Secondly, in order to fabricate devices using SMMs, new technologies must be developed; so far there are only a few examples of SMMs for which surface deposition and addressing of single molecules has been explored. One can envision temperature not being an issue if the physical properties of the new SMMs should out-perform the classical magnets used today. Still, the issue of depositing and addressing a single molecule on a surface remains a great challenge for scientists working in the field.

The promise of the ultimate miniaturization of information storage and processing devices using SMMs has driven many researchers' efforts in obtaining new improved examples of SMMs. In particular, the main goal has been to obtain SMMs with higher working temperatures, but there are still many different ways in which researchers report the success of new SMMs; a useful parameter would be the blocking temperature. The blocking temperature, T_b, the maximum temperature at which the SMM is functional, should be the temperature at which magnetization hysteresis *vs.* field is observed. The use of the blocking temperature is greatly hampered due to the fact that its value greatly depends on the sweep rate of the magnetic field during the measurement and on the experiment used to measure it, so when comparing blocking temperature values one should be extremely careful. When characterizing SMMs, the effective barrier for reversal of the magnetization, U_{eff}, is most often reported in the literature. This is also called the anisotropy barrier and it is the energy needed to transform the SMM into a simple paramagnet. U_{eff} is the most popular parameter used to characterise SMMs, mainly due the phenomenon of quantum tunnelling of the magnetization, of particular importance for 3d–4f SMMs. For a complex to be a good SMM with a high blocking temperature, U_{eff} must be large. Several researchers have proposed ways in which to normalise the parameters that should be reported for each new SMM. Long and co-workers proposed that the temperature at which 1/2 width hysteresis is observed should be reported, while Sessoli and co-workers proposed to define the

Departament de Química Inorgànica i Institut de Nanociència i Nanotecnologia, Universitat de Barcelona. Av. Diagonal 645, 08028 Barcelona, SPAIN.
E-mail: esanudo@ub.edu

blocking temperature as the temperature at which the magnetisation relaxes in 100 s. However, neither of these two definitions is widely used by scientists in the field and U_{eff} is still the parameter that is usually reported. In part, this is due to the fact that most reported SMMs do not display hysteresis of the magnetization above 1.8 K, the lower limit in temperature for commercial SQUID magnetometers, thus access to lower temperatures is required to perform magnetisation *vs.* field hysteresis measurements to obtain T_b. The Mn_{12} family of SMMs, with an $S = 10$ ground state, were the SMMs with the highest blocking temperatures ($T_b = 3.5$ K) and U_{eff} values up to 74 K[2] until 2007, when Brechin and co-workers reported a Mn_6 complex with a record U_{eff} of 86.4 K and $S = 12$.[3] Thus, many SMMs have been reported since Mn_{12}Ac, but reported working temperatures still remain in the liquid helium range. If anisotropy barriers are compared the case is similar, and the reported values are not that much greater than that of Mn_{12}Ac. The anisotropy barrier for the reversal of the magnetization in transition metal SMMs depends on two properties: the total spin of the molecule, S, and the Ising-type anisotropy, gauged by the zero-field splitting parameter, D, defined as $U_{eff} = S^2|D|$ or $U_{eff} = (S^2 - 1/4)|D|$ for integer and half-integer spins, respectively. This knowledge has been used to design improved SMMs based on two strategies: raising S and increasing the anisotropy of the molecule. Increasing S by introducing stronger ferromagnetic coupling has been achieved in several examples, but with more complex structures, a large S value has not been accompanied by a large molecular anisotropy: examples are Mn_{18},[4] Mn_{21},[5] Mn_{84}[6] or Mn_{19}.[7] In particular the latter, Mn_{19}, possesses the record spin of 83/2 for a molecular cluster, but it lacks anisotropy and thus it is not an SMM. The focus is set now on increasing the magnetic anisotropy of the prepared complexes in order to improve their SMM properties.

In this context lanthanides seem a great choice for obtaining better SMMs: the lanthanide ions (and also the actinides) have huge single-ion anisotropies. In 2003, the first mononuclear SMMs were reported and they contained a lanthanide ion. Ishikawa and co-workers reported mononuclear TBA[$Ln(Pc)_2$] complexes,[8] which were the first mononuclear SMMs and the first lanthanide SMMs. The TBA[$Ln(Pc)_2$] complex displayed frequency-dependent ac out-of-phase peaks as high as 40 K and had energy barriers of $U_{eff} = 230$ K and $U_{eff} = 28$ K with Ln = Tb and Ln = Dy, respectively. After these groundbreaking developments, the quest for improved SMMs took a new approach: to combine 3d and 4f metal centres in the same complex to obtain SMMs that would have higher working temperatures than those obtained for 3d metal SMMs.

As of August 2014, in the Cambridge Crystallographic Database there are 1632 hits for Ln–oxo–3d (3d = V, Cr, Mn, Fe, Co, Ni, Cu) compounds, including MOFs, polymeric structures and salts. Of these, about 387 research papers report heterometallic molecular complexes containing 3d metals and lanthanide ions; in many instances the paper reports several crystal structures or a family of 3d–4f complexes where usually the lanthanide is changed in each complex. In nearly 100 of these publications, 3d–4f SMMs are reported, and it is usually the Tb(III) and Dy(III) complexes that display SMM properties. This perspective gives an overview of what researchers want to achieve by preparing 3d–4f SMMs, the most significant results obtained so far and the challenges still ahead of us.

3d–4f SMMs: exploiting the magnetic properties of the 4f ions

If controlling spin is a hard task for experimental chemists, controlling the anisotropy of a high nuclearity complex is even more complicated. Initially, complexes of the more anisotropic transition metals, known to display strong axial anisotropy, such as Mn(III), Co(II) and Ni(II), were investigated, and still are, as a means to obtain better SMMs. However, in the early 2000s the search for 3d–4f SMMs became an important trend, with the goal of improving the anisotropy of the obtained species and thus obtaining better SMM properties. The lanthanide ions are well known for having strong spin–orbit coupling, their magnetic properties ruled by the quantum number, J, which has the maximum value of $|L + S|$ for lanthanides with more than half-filled f shells (Tb, Dy, Ho, Er, Tm, Yb, Lu) and the minimum value of $|L - S|$ for lanthanides with less than half-filled f shells (Ce, Pr, Nd, Pm, Sm, Eu). The number of unpaired electrons has little impact on the magnetic moment of the lanthanide ion and those with large m_J values of the ground state are the ones with stronger magnetic moments. The ground state bistability characteristic of an SMM arises in lanthanide ions from the m_J sublevels of the $^{2S+1}L_J$ term. The most common lanthanide ions used to obtain SMMs are terbium(III) and dysprosium(III), but also erbium(III), samarium(III), ytterbium(III), gadolinium(III) and holmium(III) have been used. As Ishikawa showed for the Tb and Dy sandwich phthalocyanin complexes reported in 2003,[8] in lanthanide SMMs the energy barrier is defined by the spin and angular momentum of a single lanthanide placed in a ligand field giving the largest $|Jz|$, the lowest energy, and a large energy gap to the next sublevels. Long and Rinehart proposed simple rules in order to exploit the lanthanides' single-ion anisotropy for designing 4f SMMs.[9] According to their theory, to maximize the anisotropy of oblate ions (Ce(III), Pr(III), Nd(III), Tb(III), Dy(III) and Ho(III)) the crystal field should be such that the ligand electrons are concentrated above and below the xy plane. On the other hand, for prolate ions (Pm(III), Sm(III), Er(III), Tm(III) and Yb(III)) an equatorial coordination geometry is preferred. Many of the reported 4f SMMs follow this prediction, and it is particularly useful for mononuclear lanthanide SMMs. This simple qualitative way of predicting SMM behaviour could also be used to ascertain whether a lanthanide ion in a 3d–4f complex will contribute strongly to the complex anisotropy, and thus, to the SMM properties of the 3d–4f species. However, this must only be considered in a very qualitative manner. Given the difficulties in factoring out all of the contributions to a polynuclear complex's magnetic anisotropy, the relationship between the ligand arrangement around the

lanthanide ion in a 3d–4f polynuclear complex and the complex's axial anisotropy will not be as straightforward as with mononuclear lanthanide SMMs. Ideally, the most anisotropic 3d metals should be combined with the right lanthanide to obtain new SMMs: the anisotropy of the 3d–4f complex will be a combination of the single-ion anisotropies of all the paramagnetic metal centres involved. A huge advantage of the lanthanide ions is the possibility of preparing families of complexes in which the properties of the 3d metal core can be checked, for example using the diamagnetic Y(III) or the lanthanides La(III) or Lu(III), with similar ionic radii, or the isotropic Gd(III). In this way, one can check the contribution to the SMM property from the 3d metals in the molecule; for example, the family of complexes **5** in Table 1,[10] where the **5** (La) without 4f electrons or anisotropy provided by the lanthanide ion is an SMM, indicating that the $[Mn_6]$ core of the molecule is the main contribution to the anisotropy. Using a diamagnetic 3d metal analogue might be feasible, as many researchers have done in the past for different reasons. Metals in the oxidation state +3 can be replaced by Ga(III)[11] and metals in the oxidation state +2 can be replaced by diamagnetic Zn(II), however, these are more complicated reactions than replacing a lanthanide for Gd(III) or La(III), and one must not take for granted that it will be possible to study the Ln(III) in the cluster environment without the 3d electrons or anisotropy of the 3d single ions.

So far, the magnetic coupling between 4f and 3d metals has not been mentioned. It has been tacitly understood that for better SMMs the magnetic coupling between the metal centres in the complex should be strong and ferromagnetic to provide isolated ground states and avoid mixing of low-lying excited states that can provide ways for QTM to occur. Perhaps this is one of the biggest problems of 3d–4f complexes as SMMs: the magnetic coupling between transition metals and lanthanide ions is generally weak or very weak. Monoatomic oxo bridges are the surest way to enforce the strongest possible coupling. Usually, 3d–4f exchange constants have values below 5 K. A great tool to elucidate 3d–4f magnetic coupling is the software

Table 1 3d–4f SMMs. The effective barriers measured with an applied dc field have the field value in Oe in parentheses

	Formula	U_{eff} (K)	T_b (K)	Ref.
1	$[CuLLn(hfac)_2]_2$ (Ln = Tb, Dy)	2.1	1.2	19
2	$[Dy_6Mn_6(H_2shi)_4(Hshi)_2(shi)_{10}(MeOH)_{10}(H_2O)_2]$			20
3	$[Mn_{11}Dy_4O_8(OH)_6(OMe)_2(O_2CPh)_{16}(NO_3)_5(H_2O)_3]$	9.3		21
4	$[Mn_{18}DyO_8(Cl)_{6.5}(N_3)_{1.5}(HL)_{12}(MeOH)_6]Cl_3$		0.5	23
5	$[PrNH_2]_3[Mn_6LnO_3(OMe)_3(SALO)_6(SALOH)_3]$ (Ln = La, Dy, Tb)	6; 1.3		10
6	$[M_2(L)_2(PhCOO)_2Dy_2(hfac)_4]$ (M = Zn, Co)	47.9; 8.8		26
7	$[Co_2Dy_2(OMe)_2(teaH)_2(Piv)_6]$	51; 127		29
8	$[Dy_2Co_2(OMe)_2(L)_2(OOCPh)_4(MeOH)_4](NO_3)_2$ (L = teaH, dea, mdea, bdea)	87, 104		31
9	$[Dy_2Co_2(OMe)_2(L)_2(OOCPh)_4(MeOH)_2(NO_3)_2]$ (L = mdea, tea, bdea)	79, 115		31
10	$[Dy_2Co_2(OMe)_2(teaH)_2(OOCPh)_4(MeOH)_2(NO_3)_2]$	88		32
11	$[Cr_2Dy_2(OMe)_2(Rdea)_2(acac)_4(NO_3)_2]$ (R = Me, Et, *t*Bu)	34, 37, 41	1.8, 2.2, 2.2	33
12	$[Cr_2Dy_2(OMe)_2(O_2CPh)_4(mdea)_2(NO_3)_2]$	77	2.2	33
13	$[Dy_2Mn_2(OH)_2(CymCOO)_8(THF)_4]$			34
14	$[Ni_2Dy_2(L)_4(NO_3)_2(S)_2]$ (S = MeOH, DMF)	21.3; 18.5	4.2; 3.2	35
15	$[Co_2Dy_2(L)_4(NO_3)_2(THF)_2]$	82	3	36
16	$[Mn_5Ln_4(O)_6(mdea)_2(mdeaH)_2(Piv)_6(NO_3)_4(H_2O)_2]$ (Ln = Dy, Ho, Y)	38.6	1.9	37
17	$[Mn_{21}DyO_{20}(OH)_2(tBuCOO)_{20}(HCOO)_4(NO_3)_3(H_2O)_7]$	74	3	38
18	$[Dy_{10}Co_2(L)_4(MeCOO)_{16}(SCN)_2(MeCN)_2(H_2O)_4(OH)_6]\cdot 2Co(SCN)_4$	4.3; 25		39
19	$[H_3O][Cu_{24}Dy_8(Ph_3CPO_3)_6(Ph_3CPO_3H)_6(MeCOO)_{12}(MeCOOH)_6(OH)_{42}(NO_3)(OH_2)_6]$	4.6	0.6	40
20	$[Mn_9Dy_8O_8(OH)_8(tea)_2(teaH)_2(teaH_2)_4(MeCOO)_4(NO_3)_2(H_2O)_4](NO_3)_7$			41
21	$[Mn_6O_3(saO)_6(MeO)_6Ln_2(MeOH)_4(H_2O)_2]$ (Ln = Tb, La)	103; 32.8	3.1; 8.7	45
22	$[Ln_2Mn_6O_3(OMe)_4(Et\text{-}saO)_6(acac)_2(S)_4]$ (Ln = Gd, S = MeOH; Ln = Tb, S = 3 MeOH 1 EtOH)	24; 46		46
23	$[Ln_6Mn_{12}O_7(OH)_{10}(MeCOO)_{14}(mpea)_8]$ (Ln = Tb, Gd)	36.6		47
24	$[Tb_6Mn_{12}O_9(OH)_8(MeCOO)_{10}(mpea)_8(mp)_2(MeOH)_2(H_2O)_2]$	19.6		47
25	$[Mn_5Tb_4O_6(mdea)_2(mdeaH)_2(Piv)_6(NO_3)_4(H_2O)_2]$	33		37
26	$[Mn_3Ln_4(mosao)_2(mosaoH)_4(piv)_4(N\text{-}mdea)_4]$ (Ln = Y, Tb)	13.83		48
27	$[LnCu_4(L)_2(OH)_4(H_2O)_8(NO_3)](ClO_4)_2$ (Ln = Tb, Sm)	25		49
28	$[(CuL)_2Tb(H_2O)(NO_3)_3]$	20.3		50
29	$[\{(CuL)_2Tb(H_2O)(NO_3)_3\}_2bpy]$	18		50
30	$[TbCu_3(H_2edte)(NO_3)](NO_3)_2$	19.3 (1000)	1.6	52
31	$[Cu_3Tb(Lbu)(NO_3)_2(MeOH)(H_2O)](NO_3)$	19		53
32	$[Cu(H_2L)(MeOH)]_2Tb(H_2O)_{0.57}(DMF)_{0.43}Fe(CN)_6$	13		54
33	$[Cu_6Tb_2(L)_4(NO_3)_3(MeCOO)_2(MeOH)_5]NO_3$	15.6		55
34	$[LCu(O_2COMe)Tb(thd)_2]$	13	0.7	56
35	$[Ln_2Ni_4L_2Cl_2(OH)_2(MeO)_2(MeOH)_6]Cl_2(ClO_4)_2$ (Ln = Tb, Y)	30		57
36	$[\{L_2Ni(H_2O)Tb(dmf)_{2.5}(H_2O)_{1.5}\}\{W(CN)_8\}]$	15		58
37	$[Fe_{12}Ln_4O_{10}(OH)_4(PhCO_2)_{24}]$ (Ln = Sm, Gd)	16	0.5	59
38	$[Mn_4Ln_4(n\text{Budea})_4(HCOO)_4(OMe)_4(OOCEt)_8(MeOH)_4]$ (Ln = Sm, Y)	12 (2000); 12	1	61
39	$\{(CO_3)_2[Zn(L)Ln(H_2O)]_2\}(NO_3)_2$ (Ln = Tb, Dy, Er, Yb)	19 (1000)		70
40	$[Zn(L)(NO_3)Ln(NO_3)_2]$ (Ln = Tb, Dy, Er, Yb)	27 (1000)		70
41	$[Ln_2Mn(C_7H_5O_2)_8]$ Ln = Tb, Dy	19, 92		73

PHI,[12] which was especially conceived to treat magnetic data for systems containing lanthanide ions, through the inclusion of spin–orbit coupling and crystal field effects, even though it is computationally demanding for high nuclearity complexes. The qualitative approach developed by Rinehart and Long[9] could be of use when excited states must be considered; the Dy(III) first excited states also have oblate-like shapes and could thus contribute to SMM behaviour in a coupled 3d–4f complex. However, that would not be the case for Tb(III) 3d–4f SMMs, since the excited terms are not oblate in shape.

Characterization of 3d–4f SMMs

As for any SMM, 3d–4f SMMs are usually characterized in their pure crystalline form using commercial SQUID magnetometers. The usual measurements of susceptibility against temperature and magnetization against field are also performed for 3d–4f SMMs. With these data, usually reported as the χT product and the reduced magnetisation, one can evaluate the magnetic coupling between the metal centres in the complex as well as the spin ground state. For 3d–4f complexes, this is by no means straightforward and in many it will not be possible to quantify the magnetic exchange. For SMMs, alternate current (ac) magnetic susceptibility is also measured. Usually a small magnetic field of 1–5 Oe that oscillates at frequencies between 1 and 1500 Hz is used to measure magnetic susceptibility over a range of temperatures. For an SMM each individual molecule has an energy barrier to be overcome in order to reverse the magnetic moment. The SMM molecules will freeze and lag behind the applied ac field resulting in a susceptibility signal with two components: one in-phase with the ac oscillating field χ', and one out-of-phase with the oscillating field χ''. The appearance of out-of-phase maxima that are frequency-dependent is the most reliable signature of SMM behaviour. A typical example is shown in Fig. 1. These experiments are usually performed by scanning the temperature and frequency domains, resulting in susceptibility *vs.* T and susceptibility *vs.* frequency plots. From the slope of the plot of $\ln\tau$ *vs.* $1/T$ one can obtain the anisotropy barrier where the graph is linear using an Arrhenius type of equation, $\tau = \tau_0 \exp(U_{eff}/kT)$. For lanthanide SMMs, a temperature-independent region is usually observed that is characteristic of fast relaxation of the magnetisation *via* quantum tunnelling (QTM). When the thermal mechanism coexists with the QTM, a curvature is seen in the Arrhenius plot of $\ln\tau$ *vs.* $1/T$. Several thermal relaxation processes can also coexist, and this can be assessed by examination of so-called Argand or Cole–Cole plots. In these plots, χ'' is plotted against χ' at a constant temperature, resulting in a semi-circular representation. When a distribution of energy barriers exists the semicircle is distorted, a Debye model applies and the parameter α gauges the distribution. Usually for SMMs this parameter has values smaller than 0.2.

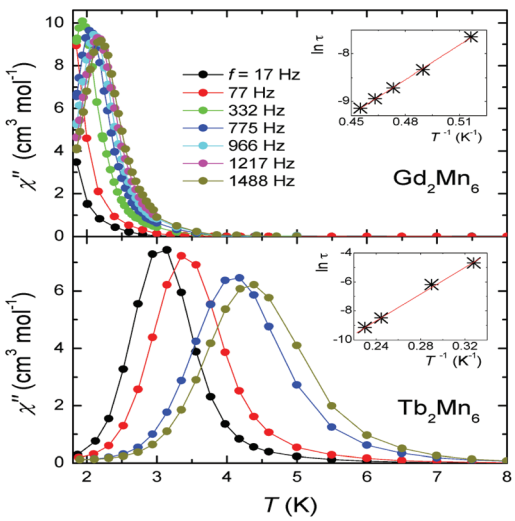

Fig. 1 Typical ac magnetic susceptibility data and Arrhenius plot for a 3d–4f SMM. Reproduced from ref. 46 with permission from the Royal Society of Chemistry.

Researchers still have a lot to learn from new lanthanide SMMs,[25] including the occurrence of multiple relaxation processes for pure SMMs,[71] and the toroidal magnetic moments in some 4f SMMs,[72] among other things. The phenomena of multiple relaxation processes and QTM also occur in transition metal SMMs.

Magnetisation *vs.* field hysteresis loops can be measured in a commercial SQUID magnetometer down to 1.8 K or using a micro-SQUID or micro-Hall probe with suitable sweep rates for the field, going down to the mK range. Due to the fact that most 3d–4f SMMs display hysteresis of the magnetisation *vs.* field at very low temperatures, when possible micro-SQUID data are reported. Blocking temperatures and anisotropy barriers can be obtained from magnetisation decay measurements, also performed using a micro-SQUID. X-ray magnetic circular dichroism (XMCD) is a technique that has been used on a few occasions to analyse the magnetic behaviour of 3d–4f complexes. XMCD is element-sensitive and can be used to probe the magnetism of each metal type in a heterometallic complex. Pedersen and co-workers published a great example in 2012, where they reported element-specific curves for a Cr–Dy complex.[13] XMCD could be exploited for evaluating the 3d–4f coupling in heterometallic complexes. Furthermore, XMCD can also be used to probe the magnetic properties of an SMM on a surface, a key and challenging step for physicists and chemists, as we reported for a Dy MOF of SMMs,[14] and as Sessoli and co-workers pioneered with their work on Mn_{12} [15] and Fe_4 [16,17] SMMs on surfaces.[18]

A wide perspective on 3d–4f SMMs

The first 3d–4f SMMs were reported in 2004: $[CuLLn(hfac)_2]_2$ (**1**, Ln = Tb, Dy; H_3L = 1-(2-hydroxybenzamido)-2-(2-hydroxy-3-methoxy-benzylideneamino)-ethane)[19] squares with the 3d and 4f metals in an alternated array reported by Matsumoto *et al.*, and the $[Dy_6Mn_6(H_2shi)_4(Hshi)_2(shi)_{10}(MeOH)_{10}(H_2O)_2]$ (**2**, H_3shi = salicylhydroxamic acid) complex, reported by Pecoraro.[20]

These complexes presented no hysteresis down to 1.8 K, the temperature limit of commercial SQUID magnetometers, but ac magnetic susceptibility studies showed out-of-phase signals, as expected for SMM behaviour. Only for **1**(Tb), $[CuLTb(hfac)_2]_2$, were the maxima of the out-of-phase signals observed above 1.8 K. In the same year, Christou and co-workers reported the first observed magnetization *vs.* field hysteresis loops for a heterometallic 3d–4f SMM,[21] the $[Mn_{11}Dy_4O_8(OH)_6(OMe)_2(O_2CPh)_{16}(NO_3)_5(H_2O)_3]$ complex, **3**. The out-of-phase ac magnetic susceptibility data showed no maxima down to 1.8 K, but magnetization *vs.* field hysteresis loops were observed using a micro-SQUID device below 1 K. The hysteresis loops were smooth, without the presence of the typical QTM steps signature of transition metal SMMs. This lack of steps in the magnetization *vs.* field hysteresis was attributed to a distribution of molecular environments or intermolecular interactions, both factors known to smooth or smear hysteresis loops in some transition metal SMMs.[22] From these three first reports one can already make a clear conclusion: the ligands used are not specific for lanthanide–3d complexes, but are the usual varied ligands used in transition metal chemistry and lanthanide chemistry. Also from only these three reports one can see how in complex **2** the dysprosium ions are close to each other and can be coupled, while in **1** and **3** the lanthanide ions are separated by the transition metals and could only couple to the transition metals.

The first results obtained seemed encouraging and efforts were doubled. In 2004 three peer reviewed research papers reported 3d–4f SMMs. From 2008 the number increased to between 10 and 16 papers each year reporting new 3d–4f SMMs. In 2014 the exponential growth in the field was reflected in more than 50 peer reviewed research papers reporting new 3d–4f SMMs. To the date of this report, 161 3d–4f SMMs have been reported. Nearly 2/3 of the reported 3d–4f SMMs contain Dy(III) as the lanthanide ion, and in most cases the coordination environment can be described as ligands above and below the plane, thus providing the ideal setting for SMM properties for an oblate ion like Dy(III). One case of a neodymium 3d–4f complex, the $[Mn_4Nd_2]$ SMM, is reported, but no hysteresis was observed.[74] The 3d metal is usually Co(II) or Mn(III), both highly anisotropic, but also Fe(III), Ni(II), Cu(II) or even the diamagnetic Co(III) and Zn(II) have been used. Worth mentioning here are the reported 3d–4f SMMs that contain Gd(III) and La(III). In these two cases the lanthanide is either isotropic (Gd(III)) or diamagnetic (La(III)). All the 3d–4f SMMs reported with these two lanthanide ions are clearly cases where the anisotropy and the SMM property are both provided for by the 3d metal part of the complex.

By design: metal substitution

As with any polynuclear coordination complex, the synthesis of 3d–4f SMMs most often follows a procedure of serendipitous self-assembly, where researchers try to provide the best reaction conditions to obtain complexes that might be new examples of SMMs. This is why there is such a rich structural diversity of 3d–4f SMMs, as is the case for transition metal SMMs. Of course the counterpart is the lack of control in the structure and properties of the prepared complexes. In the last few years the targeted substitution of a 3d metal by a lanthanide ion in a known transition metal polynuclear complex has been successfully done. This method has led to the isolation of 3d–4f complexes, where the position of the lanthanide ion could be predicted at the synthesis step. The first example was reported by Powell and co-workers in 2009,[23] when they succeeded in replacing the central Mn(II) atom of a ferromagnetically coupled $[Mn_{19}]^7$ complex, $[Mn_{19}O_8(N_3)_8(HL)_{12}(MeCN)_6]Cl_2$, with no anisotropy, for a Dy(III), to obtain $[Mn_{18}DyO_8(Cl)_{6.5}(N_3)_{1.5}(HL)_{12}(MeOH)_6]Cl_3$, (**4**). By this replacement, retaining the core topology of the cluster, the anisotropy of the complex was enhanced and the SMM property observed. Thus, the introduction of the anisotropic Dy(III) ion results in the onset of the SMM property, which was absent in $[Mn_{19}]$. Powell's complex, **4** ($Mn_{18}Dy$), provided a sandwich type of ligand environment to the Dy(III) ion and thus complex **4** displayed SMM properties. $[Mn_{19}]$ had a record $S = 83/2$ spin but lacked any appreciable anisotropy. The introduction of the Dy(III) ion in a sandwich-like crystal field provided the necessary anisotropy to observe SMM behaviour.

More recently we reported a $[Mn_7]$ species,[24] with a complex structure that was formed by three $[Mn(III)_2]$ units centred around a Mn(II) ion in a very large cavity for a transition metal. Conditions were perfect for the controlled preparation of a Mn–Ln complex. We tweaked the reaction conditions and we successfully isolated the desired complexes $[PrNH_2]_3[Mn_6LnO_3(OMe)_3(SALO)_6(SALOH)_3]$ with several lanthanide ions: La, Gd, Tb and Dy (**5**).[10] The introduction of the lanthanide ion resulted in slightly enhanced SMM properties in **5**(La) and modified SMM properties for **5**(Dy) and **5**(Tb). In **5**(Gd) the SMM properties were completely quenched, probably due to better magnetic coupling through the Gd(III) ion. In a qualitative, simple manner, this can be explained by looking at the coordination environment of the Ln(III) ion, which in the complexes **5**(Ln) was highly symmetrical, resembling a spherical arrangement of the ligands around the lanthanide, which according to Long's qualitative considerations should not provide a good crystal field for a bistable ground state for Dy(III) or Tb(III). In order to substitute a 3d metal for a lanthanide ion in a known complex there must be a metal site that is appropriate for the lanthanide. This is not straightforward and there are not many examples in the literature where controlled substitution is reported.

Dy(III) 3d–4f SMMs

Without a doubt dysprosium is the most used lanthanide in order to obtain 3d–4f SMMs. The first reports in 2004 were of 3d–Dy SMMs. 3d–Dy SMMs have been reported for cobalt, chromium, copper, iron, manganese, nickel and zinc.

In several of these examples, the 3d metals in these species are Co(III) and Zn(II), thus diamagnetic, and it can be argued whether these should be considered 3d–4f SMMs or simply lanthanide SMMs with metalloligands. We have decided to consider these species here since usually when lanthanide

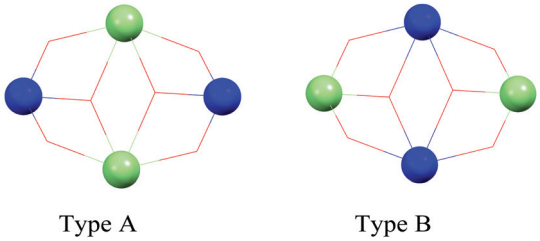

Fig. 2 Ball and stick representation of the metal–oxo core of a defective dicubane structure. The lanthanide ions are shown in green, the 3d metals are shown in blue.

SMMs are reviewed these species are not accounted for.[25] Chaudhury and co-workers propose to use diamagnetic Zn(II) ions in $[M_2(L)_2(PhCOO)_2Dy_2(hfac)_4]$ (**6**(Zn) and **6**(Co) in Table 1) to enhance the energy barrier of Dy(III) SMMs, as they show with DFT and *ab initio* calculations. This is also studied by Shanmugam and co-workers.[26,27] The record anisotropy barrier for 3d–4f SMMs belongs to a family of structurally related $[Co(III)_2Dy_2]$ complexes with a double defective cubane structure prepared using tripodal ligands, the metal–oxo core is shown in Fig. 2. This core topology is well known in transition metal chemistry, and many $Mn(II)_2Mn(III)_2$ complexes have been reported with this core that are SMMs, a review of their properties and structures can be found in Aromí and Brechin's review.[28] The highest reported anisotropy barrier for a 3d–4f SMM belongs to a member of this family of complexes, with a Type A defective dicubane core, as shown in Fig. 2. $[Co_2Dy_2(OMe)_2(teaH)_2(Piv)_6]$ (**7**, teaH = triethanolamine, Piv = pivalate)[29] displays two overlapped peaks in its out-of-phase ac magnetic susceptibility, with U_{eff} = 51 and 127 K, as shown in Fig. 3. In 2013 and in 2014, Murray and co-workers reported two families of $[Co(III)_2Dy(III)_2]$ (**8** and **9** in Table 1) with Type A metal arrangements, as shown in Fig. 2.[30,31] This work added to their previous report of a $[Ln_2Co_2(OMe)_2(teaH)_2(OOCPh)_4(MeOH)_2(NO_3)_2]$ family of complexes in 2012[32] with the same defective dicubane core. The dysprosium–cobalt analogue, $[Dy_2Co_2(OMe)_2(teaH)_2(OOCPh)_4(MeOH)_2(NO_3)_2]$ (complex **10** in Table 1), had a record energy barrier at the time of 88 K, and its ac data could be fit to a distribution of energy barriers with α = 0.25, attributed by the authors to the fact that there are two independent Dy(III) sites.

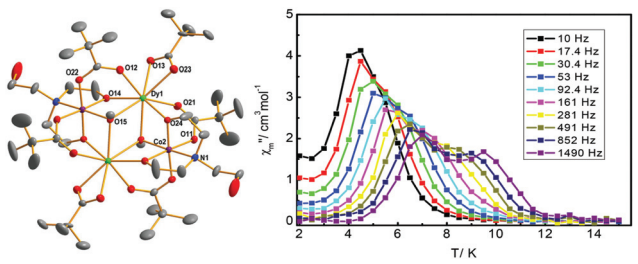

Fig. 3 Crystal structure of $[Co_2Dy_2(OMe)_2(teaH)_2(Piv)_6]$ (**6**) and out-of-phase ac susceptibility as a function of temperature, showing two overlapped peaks. Reproduced from ref. 29 with permission from the Royal Society of Chemistry.

The authors were able to evaluate the magnetic exchange between Dy(III) ions, which was weak and antiferromagnetic. QTM was suppressed in a bulk sample of complex **10** due to the weak dipolar antiferromagnetic coupling, but dilution experiments in a yttrium(III) analogue matrix showed that fast tunnelling dominated the magnetic relaxation. The same authors showed how the structurally related $[Cr_2Dy_2(OMe)_2(Rdea)_2(acac)_4(NO_3)_2]$ (Rdea = R-diethanolamine; **11**(Me) R = methyl, **11**(Et) R = ethyl or **11**(*t*Bu) R = *tert*-butyl) and $[Cr_2Dy_2(OMe)_2(mdea)_2(O_2CPh)_4(NO_3)_2]$ (**12**), with a Type A defective dicubane core as shown in Fig. 2, had large anisotropy barriers and long relaxation times compared to the Co(III) analogues due to the significant magnetic interaction between the 3d metal, Cr(III), and the lanthanide, which suppresses QTM.[33] These Cr–Dy SMMs, **11**(Me), **11**(Et), **11**(*t*Bu) and **12**, display hysteresis of the magnetization *vs.* applied field at temperatures as high as 2.2. K.

This core topology can also be found in the family $[Ln_2Mn_2(OH)_2(CymCOO)_8(THF)_4]$ (Ln = Dy **13**, Ho; Cym = $(\mu_5\text{-}C_5H_4)Mn(CO)_3$) where only the dysprosium analogue presents SMM properties.[34] In 2011 Powell and co-workers reported the Type B defective dicubane complexes $[Ni_2Ln_2(L)_4(NO_3)_2(S)_2]$ (Ln = Dy **14**(S), Tb; L = 2-(2-hydroxy-3-methoxy-benzylideneamino)phenol; S = MeOH and DMF)[35] where the two dysprosium complexes, **14**(MeOH) and **14**(DMF) are SMMs and the blocking temperature seems to be modulated by the coordination environment around the Ni(II) ions. The structure of these complexes is somewhat different from the SMMs reported by Murray and co-workers; now the dysprosium ions are not part of the central $[M_2O_2]$ unit, but at the tips of the molecule, resulting in two fairly well separated ions, nearly magnetically independent. In 2012 the same group reported $[Co_2Dy_2(L)_4(NO_3)_2(THF)_2]$ (**15**),[36] a Type B defective dicubane, which was also a SMM. Cobalt is in the oxidation state Co(II), and is paramagnetic. The authors show how single-ion blocking of the Dy(III) ions occurs at higher temperatures with a crossover to molecular exchanged-based blocking at low temperatures. For **15** there are two differentiated thermally-activated regimes with effective barriers of 82 and 11 K. Hysteresis loops were clearly observed up to 3 K. In this very interesting paper the authors unambiguously assign the large energy barrier to the relaxation of the Dy(III) ions and the low temperature behaviour to the exchange-blocked relaxation where the 3d–4f coupling dominates.

A number of higher nuclearity 3d–4f complexes have been reported, many of them SMMs with diverse structures and ligands. Most of these have relatively small energy barriers. An exception is an enneanuclear complex $[Mn_5Dy_4O_6(mdea)_2(mdeaH)_2(Piv)_6(NO_3)_4(H_2O)_2]$ (**16**(Dy)) reported by Powell *et al.*; the complex possesses an energy barrier of 38.6 K and displays magnetisation *vs.* field hysteresis loops up to 1.9 K.[37] The Tb(III), Ho(III) and Y(III) (**16**(Tb), **16**(Ho) and **16**(Y)) analogues are also SMMs, but with smaller energy barriers. The diamagnetic

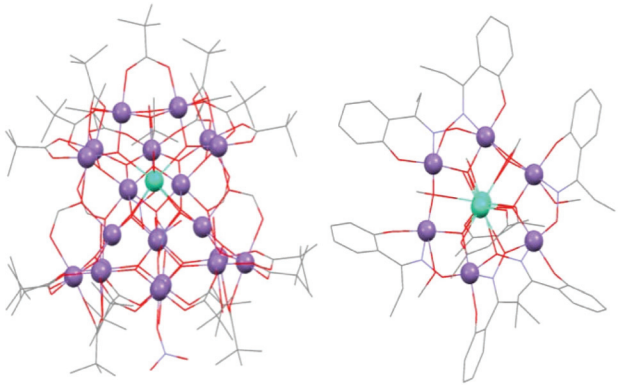

Fig. 4 Crystal structures of some 3d–4f SMMs: (left) $[Mn_{21}DyO_{20}(OH)_2(tBuCOO)_{20}(HCO_2)_4(NO_3)_3(H_2O)_7]$ (**17**) from ref. 38; (right) $[Mn_6O_3(saO)_6(MeO)_6Tb_2(MeOH)_4(H_2O)_2]$ (**21**(Tb)) from ref. 45. Manganese: purple, lanthanide: cyan, carbon: grey, oxygen: red, nitrogen: blue.

Y(III) analogue highlights the fact that the Mn_5 unit also contributes to the SMM behaviour.

The $[Mn_{21}DyO_{20}(OH)_2(tBuCOO)_{20}(HCO_2)_4(NO_3)_3(H_2O)_7]$ complex (**17**) shown in Fig. 4, reported by Christou and co-workers in 2011, also shows hysteresis of the magnetization up to 3 K and has a large energy barrier of 74 K.[38] In complex **17** a single Dy(III) is at one vertex of a $[M_4O_4]$ cubane, which is surrounded by a Mn–O core that is probably a strong contributor to the SMM properties. The 3d–4f SMM containing the largest number of Dy(III) ions is complex **18** with ten Dy(III) and two cobalt ions, $[Dy_{10}Co_2(L)_4(MeCOO)_{16}(SCN)_2(MeCN)_2(H_2O)_4(OH)_6]\cdot 2Co(SCN)_4$, reported in 2011 by Tang and his group.[39] Complex **18** contains ten dysprosium ions and two Co(II) in a wheel-like arrangement. Below 10 K the authors report slow relaxation with a crossover from single-ion relaxation to the exchanged coupled system due to the Dy(III) centres. Two complexes have been reported with eight dysprosium ions. $[H_3O][Cu_{24}Dy_8(Ph_3CPO_3)_6(Ph_3CPO_3H)_6(MeCOO)_{12}(MeCOOH)_6(OH)_{42}(NO_3)(OH_2)_6]$ (**19**) was reported in 2010 by Winpenny and co-workers.[40] The Gd(III) analogue is not an SMM, thus the anisotropy is provided by the eight dysprosium ions. As usual for very large complexes, the blocking temperature is very low (0.6 K) and the magnetization *vs.* field hysteresis loops are smooth. The same year Murray and co-workers reported complex **20** with nine Mn(III) and eight dysprosium ions, $[Mn_9Dy_8O_8(OH)_8(tea)_2(teaH)_2(teaH_2)_4(MeCOO)_4(NO_3)_2(H_2O)_4](NO_3)_7$.[41] Complex **20** is an SMM but no maxima in the ac susceptibility were observed. Again, the largest nuclearity complexes fail to provide the best magnetic properties. In 2015 Tang and co-workers reported Mn(II)–Ln_2 SMMs, with the Dy(III) analogue, **41**(Dy), displaying a large U_{eff} = 92 K.[73]

Tb 3d–4f SMMs

Terbium(III) is the lanthanide ion that has provided the mononuclear SMM complexes with record effective energy barriers[42–44] due to the large separation of the m_J sublevels and the large anisotropy characteristic of terbium(III). However, terbium is a non-Kramer's ion and the ground state will only be bi-stable in axial-symmetry ligand fields. Thus, there are many fewer Tb(III) SMMs reported than Dy(III) SMMs. For 3d–4f SMMs this picture still holds: for every two 3d–Dy SMMs reported complexes there is only one 3d–Tb SMM. The terbium analogues of 3d–Dy SMMs most of the time do not display SMM properties or are worse SMMs than their dysprosium analogues. SMMs containing Tb have been reported mostly for copper and manganese, but also with nickel, cobalt, iron and chromium. The ones with the highest energy barriers are manganese–terbium complexes. In 2011 Dehnen and co-workers reported the octanuclear complex $[Mn_6O_3(saO)_6(MeO)_6Tb_2(MeOH)_4(H_2O)_2]$ (**21**(Tb)) with an energy barrier of 103 K.[45] This complex displayed a high blocking temperature of 3.1 K. The lanthanum analogue, **21**(La) was also an SMM with a large blocking temperature and relatively large energy barrier of 32 K. Brechin and co-workers reported the same year complex **22**(Gd), $[Gd_2Mn_6O_3(OMe)_4(Et\text{-}sao)_6(acac)_2(MeOH)_4]$, with a similar core, but different ligands and an energy barrier of 24 K.[46] The energy barrier was also high for the terbium complex **22**(Tb), U_{eff} = 46 K. In this case clearly the anisotropy of the terbium ion has actually boosted the SMM properties of the $[Mn_6]$ unit, showing how the right combination of anisotropic 3d metal and anisotropic lanthanide can lead to better, improved SMMs. The high nuclearity, high symmetry (D_2) complex **23**(Tb) reported by Tong and co-workers, $[Tb_6Mn_{12}O_7(OH)_{10}(OAc)_{14}(mpea)_8]$,[47] has an energy barrier of U_{eff} = 36.6 K. A related complex, which differs in some of the terminal ligands and the orientation of the two related $[Ln(III)_3]$ units, complex **24**, $[Tb_6Mn_{12}O_9(OH)_8(OAc)_{10}(mpea)_8(mp)_2(MeOH)_2(H_2O)_2]$, has lower symmetry ($C_1$) and a smaller energy barrier value of 19.6 K. In this particular case, the dysprosium analogue **23**(Dy) has a smaller anisotropy barrier. Complex **25**, $[Mn_5Tb_4O_6(mdea)_2(mdeaH)_2(Piv)_6(NO_3)_4(H_2O)_2]$, reported by Powell and co-workers with a core of two distorted $[Mn(IV)Mn(III)Tb_2O_4]$ cubanes sharing a Mn(IV) vertex, has an energy barrier of the same order (33 K).[37] Another example with an even smaller anisotropy barrier is complex **26**(Tb), $[Mn_3Tb_4(mosao)_2(mosaoH)_4(piv)_4(N\text{-}mdea)_4]$, consisting of two triangles of $[Mn(III)Tb_2]$ linked to a central Mn(II) atom, the analogue with diamagnetic Y, **26**(Y), has an energy barrier of 13.8 K generated by the anisotropy and spin of the manganese unit.[48]

There are several 3d–Tb SMMs synthesized with Cu, the most relevant is complex **27**, $[TbCu_4(L)_2(OH)_4(H_2O)_8(NO_3)](ClO_4)_2$, with U_{eff} = 25 K, a tetragonal pyramid with a large and flexible ligand bis(-carboxyethyl)isocyanurate.[49] On the other hand, we can see an example of a family of trinuclear $[Cu_2Tb]$ complexes like $[(CuL)_2Tb(H_2O)(NO_3)_3]$ (**28**) or $[\{(CuL)_2Tb(H_2O)(NO_3)_3\}_2bpy]$ (**29**) with different assemblies, showing values of anisotropy barrier between 18 K and 23 K.[50] A one-dimensional chain of units like that of complexes **28** and **29** behaves as a single-chain magnet (SCM).[50,51] Two more examples of Cu–Tb SMMs are complex **30**, $[TbCu_3(H_2edte)(NO_3)](NO_3)_2$,[52] or complex **31**, $[Cu_3Tb(L^{bu})(NO_3)_2(MeOH)(H_2O)](NO_3)$, with an hexaimine macrocycle ligand.[53] Complex **32** is a rare example

of a heterotrimetallic coordination complex of formula $[Cu(H_2L)(MeOH)]_2Tb(H_2O)_{0.57}(DMF)_{0.43}Fe(CN)_6$ exhibiting an energy barrier of 13 K.[54] Some other SMMs reported in the reference list are an octanuclear complex $[Cu_6Tb_2(L^3)_4(NO_3)_3(OAc)_2(MeOH)_5]NO_3$, complex **33**, described as an oblate wheel that has an energy barrier of 15.6 K[55] or complex **34**, a dinuclear Cu–Tb complex, $[LCu(O_2COMe)Tb(thd)_2]$, with a Schiff base ligand with U_{eff} = 13 K.[56]

The complex $[Tb_2Ni_4L_2Cl_2(OH)_2(MeO)_2(MeOH)_6]Cl_2(ClO_4)_2$, **35**(Tb), is a defective dicubane complex with Schiff base ligands. Complex **35**(Tb) exhibits an anisotropy barrier of 30 K. The magnetic data obtained for the Ni–Y(III) analogue **35**(Y) demonstrated that the 4f metal contribution to the SMM properties was dominant.[57] Complex **36** is another rare heterotrinuclear 3d–4f–5d complex containing tungsten,[58] $[\{LMe_2Ni(H_2O)Tb(dmf)_{2.5}(H_2O)_{1.5}\}\{W(CN)_8\}]$, showing an anisotropy barrier of 15 K. It is worth pointing out that none of the reported 3d–Tb(III) SMMs report magnetization *vs.* field hysteresis loops above 2.0 K.

Sm, Ho, Er and Yb 3d–4f SMMs

Even though dysprosium and terbium are undoubtedly the two lanthanide ions that have provided better SMMs, there are some interesting examples with other lanthanide ions. Samarium, with a less than half-filled shell and the smallest J at ground state is rarely present in SMMs. According to the observations of Long and Rinehart, a mostly equatorial arrangement of ligands would be required to provide a bistable ground state for an isolated Sm(III) ion. This ligand arrangement is not very common. In 2010 Bu and co-workers reported the first Sm–3d SMM, $[Fe_{12}Sm_4O_{10}(OH)_4(PhCO_2)_{24}]$ (**37**(Sm)).[59] Complex **37**(Sm) contained twelve Fe(III) ions and four Sm(III) ions, with an effective barrier of 16 K and a blocking temperature of 0.5 K. In **37**(Sm) each Sm(III) ion interacts with five iron centres and one samarium *via* monoatomic oxo bridges. The $[Fe_{12}]$ unit of the cluster possesses a large spin ground state, but **37**(Gd) is not an SMM. The large spin of the $[Fe_{12}]$ part of the cluster combined with a ligand arrangement around the samarium in an unusual muffin-like geometry with five ligands around the Sm(III) ion in an equatorial fashion results in a bistable ground state. Since the magnetic moment of samarium is not large, even with the ideal ligand field, the $[Fe_{12}Sm_4]$ complex **37**(Sm) is not a very good SMM. In 2014 the same group reported new members of the same family of $[Fe_{12}Sm_4]$ SMMs, with similar magnetic properties.[60] In 2010 Powell and co-workers reported a family of $[Mn(III)_4Ln(III)]$ complexes, **38**. **38**(Sm), $[Mn_4Sm_4(n\text{Budea})_4(HCOO)_4(OMe)_4(OOCEt)_8(MeOH)_4]$, is an SMM with an energy barrier of 12 K when an applied dc field of 2000 Oe is used to suppress QTM.[61] The yttrium analogue **38**(Y) also presents slow relaxation of the magnetization, highlighting the importance of the $[Mn(III)_4]$ part of the cluster in the slow relaxation behaviour. The complex **27**(Sm), $[SmCu_4(L)_2(OH)_4(H_2O)_8(NO_3)][(ClO_4)_2$, reported in 2012 as an analogue to **27**(Tb), is also a SMM.[49]

Two papers report 3d–Er SMMs[62,63] and there are eight 3d–Ho SMMs.[34,57,64–68,69] All of them display very small energy barriers and no reported blocking temperatures. Some of these are part of families of SMMs, where usually the Dy and Tb analogues display better SMM properties.

Two ytterbium 3d–4f SMMs, **39** and **40** in Table 1, were reported in 2014 by Brechin *et al.*[70] These were the first two 3d–4f SMMs of Yb(III), but the 3d metal was Zn(II), diamagnetic. Ac out-of-phase susceptibility peaks were observed when applying a 1000 Oe dc field, something usual for Yb(III) SMMs. The interest in these species was focused on a combination of SMM and luminescent properties, associated to Yb(III).

Challenges ahead and concluding remarks

The biggest challenge still remains, to raise the blocking temperature of new SMMs, no matter whether we talk about transition metals, 4f or 3d–4f SMMs. We have included here some complexes that are claimed as SMMs but for which no maxima in the out-of-phase ac magnetic susceptibility or hysteresis of the magnetization *vs.* field are reported. Clearly, the limited access to experiments at temperatures below 2 K is an obstacle in this respect. However, we expect that when new 3d–4f SMMs with higher blocking temperatures are reported, this fact will cease to be a problem and there will be less ambiguity as to the physical properties of reported species: both ac magnetic susceptibility out-of-phase maxima and magnetization *vs.* field hysteresis should be observed to claim a complex is an SMM. With lanthanide SMMs the effective energy barriers have been greatly increased, up to hundreds of Kelvin in several mononuclear SMMs, Tb–phthalocyanine derivatives, pure or doped in diamagnetic yttrium matrices,[25] but this has not been accompanied by a real increase in blocking temperatures, thus hampering the potential application of lanthanide SMMs. This problem might be overcome by 3d–4f SMMs. Several examples report large effective energy barriers (at least of the order of those reported for 3d SMMs) that are in a few cases accompanied by relatively high blocking temperatures, such as those reported by Murray and co-workers for $[Cr_2Dy_2]$ SMMs, with T_b = 2.2 K, and particularly relevant, the $[Mn_6Tb_2]$ reported by Dehnen and co-workers with U_{eff} = 103 K and T_b = 3.5 K.[33,45] The Cr(III)–Dy(III) significant magnetic interaction is claimed to be the key factor in quenching QTM and it is directly related to the anisotropy barrier, thus opening up a challenging new route to control SMM properties of Cr(III)–Dy(III) ions. Could this be exploited for other 3d–4f SMMs? It is still a big synthetic challenge to prepare 3d–4f complexes with strong magnetic coupling between the 3d and 4f ions, but this might be a great goal to have in mind. The synthetic methods clearly offer a rich variety of products, with different levels of control in the design of the prepared complexes. There is not a clear picture of preferred ligands to prepare 3d–4f SMMs, and complexes are reported with all kinds of ligands, but polyalcoxo ligands and Schiff bases of salicylaldehyde appear in many of the reported complexes.

The advances in the theoretical understanding of the magnetic properties of the lanthanide ions and their 3d–4f complexes are still lagging behind the advances in the synthesis of new complexes. There is still a lot to learn about heterometallic 3d–4f complexes, especially about the magnetic coupling between 3d and 4f metals. We strongly believe the study of 3d–4f interactions as it becomes more common, even in dinuclear model complexes, will provide good ideas for the design of new 3d–4f SMMs. From the knowledge base of 3d–4f SMMs reported up to 2014, dysprosium seems to be the best lanthanide to provide 3d–4f SMMs. Furthermore, two main trends of design of new 3d–4f SMMs have emerged as the most plausible to provide better 3d–4f SMMs in the near future: isolated lanthanide ions with a 3d metalloligand, as in the [$Mn_{21}Dy$] reported by Christou and co-workers,[38] with T_b = 3.0 K; or 3d–4f complexes with strong magnetic coupling between the metals to suppress QTM. Also a combination of these approaches emerges as a good option: a 3d–4f SMM with strong coupling between a unique lanthanide ion and a 3d metalloligand with large S that would help in quenching the QTM, thus increasing the blocking temperature.

Acknowledgements

ECS and LRP acknowledge the financial support from the Spanish Government, (Grant CTQ2012-32247).

Notes and references

1 R. Sessoli, H.-L. Tsai, A. R. Schake, S. Wang, J. B. Vincent, K. Folting, D. Gatteschi, G. Christou and D. N. Hendrickson, *J. Am. Chem. Soc.*, 1993, **115**, 1804–1816.
2 N. E. Chakov, S. Lee, A. G. Harter, P. L. Kuhns, A. P. Reyes, S. O. Hill, N. S. Dalal, W. Wernsdorfer, K. A. Abboud and G. Christou, *J. Am. Chem. Soc.*, 2006, **128**, 6975–6989.
3 C. J. Milios, A. Vinslava, W. Wernsdorfer, S. Moggach, S. Parsons, S. P. Perlepes, G. Christou and E. K. Brechin, *J. Am. Chem. Soc.*, 2007, **129**, 2754–2755.
4 E. K. Brechin, C. Boskovic, W. Wernsdorfer, J. Yoo, A. Yamaguchi, E. C. Sanudo, T. R. Concolino, A. L. Rheingold, H. Ishimoto, D. N. Hendrickson and G. Christou, *J. Am. Chem. Soc.*, 2002, **124**, 9710–9711.
5 E. C. Sañudo, W. Wernsdorfer, K. A. Abboud and G. Christou, *Inorg. Chem.*, 2004, **43**, 4137–4144.
6 A. J. Tasiopoulos, A. Vinslava, W. Wernsdorfer, K. A. Abboud and G. Christou, *Angew. Chem., Int. Ed.*, 2004, **43**, 2117–2121.
7 A. M. Ako, I. J. Hewitt, V. Mereacre, R. Clérac, W. Wernsdorfer, C. E. Anson and A. K. Powell, *Angew. Chem., Int. Ed.*, 2006, **45**, 4926–4929.
8 N. Ishikawa, M. Sugita, T. Ishikawa, S.-Y. Koshihara and Y. Kaizu, *J. Am. Chem. Soc.*, 2003, **125**, 8694–8695.
9 J. D. Rinehart and J. R. Long, *Chem. Sci.*, 2011, **2**, 2078–2085.
10 M. Ledezma-Gairaud, L. Grangel, G. Aromí, T. Fujisawa, A. Yamaguchi, A. Sumiyama and E. C. Sañudo, *Inorg. Chem.*, 2014, **53**, 5878–5880.
11 E. C. Sañudo, C. A. Muryn, M. A. Helliwell, G. A. Timco, W. Wernsdorfer and R. E. P. Winpenny, *Chem. Commun.*, 2007, 801–803.
12 N. F. Chilton, R. P. Anderson, L. D. Turner, A. Soncini and K. S. Murray, *J. Comput. Chem.*, 2013, **34**, 1164–1175.
13 J. Dreiser, K. S. Pedersen, C. Piamonteze, S. Rusponi, Z. Salman, M. E. Ali, M. Schau-Magnussen, C. A. Thuesen, S. Piligkos, H. Weihe, H. Mutka, O. Waldmann, P. Oppeneer, J. Bendix, F. Nolting and H. Brune, *Chem. Sci.*, 2012, **3**, 1024–1032.
14 M. Chen, E. C. Sañudo, E. Jiménez, S.-M. Fang, C.-S. Liu and M. Du, *Inorg. Chem.*, 2014, **53**, 6708–6714.
15 M. Mannini, P. Sainctavit, R. Sessoli, C. Cartier dit Moulin, F. Pineider, M.-A. Arrio, A. Cornia and D. Gatteschi, *Chem. – Eur. J.*, 2008, **14**, 7530–7535.
16 M. Mannini, F. Pineider, C. Danieli, F. Totti, L. Sorace, P. Sainctavit, M. Arrio, E. Otero, L. Joly, J. C. Cezar, A. Cornia and R. Sessoli, *Nature*, 2010, **468**, 417–421.
17 L. Malavolti, V. Lanzilotto, S. Ninova, L. Poggini, I. Cimatti, B. Cortigiani, L. Margheriti, D. Chiappe, E. Otero, P. Sainctavit, F. Totti, A. Cornia, M. Mannini and R. Sessoli, *Nano Lett.*, 2015, **15**, 535–541.
18 R. Sessoli, M. Mannini, F. Pineider, A. Cornia and P. Sainctavit, *Magnetism and Synchrotron Radiation*, Springer Berlin Heidelberg, Berlin, Heidelberg, 2010, vol. 133.
19 S. Osa, T. Kido, N. Matsumoto, N. Re, A. Pochaba and J. Mrozinski, *J. Am. Chem. Soc.*, 2004, **126**, 420–421.
20 C. M. Zaleski, E. C. Depperman, J. W. Kampf, M. L. Kirk and V. L. Pecoraro, *Angew. Chem., Int. Ed.*, 2004, **43**, 3912–3914.
21 A. Mishra, W. Wernsdorfer, K. A. Abboud and G. Christou, *J. Am. Chem. Soc.*, 2004, **126**, 15648–15649.
22 E. C. Sañudo, W. Wernsdorfer, K. A. Abboud and G. Christou, *Inorg. Chem.*, 2004, **43**, 4137–4144.
23 A. M. Ako, V. Mereacre, R. Clérac, W. Wernsdorfer, I. J. Hewitt, C. E. Anson and A. K. Powell, *Chem. Commun.*, 2009, 544–546.
24 M. Ledezma-Gairaud, L. W. Pineda, G. Aromí and E. C. Sañudo, *Polyhedron*, 2013, **64**, 45–51.
25 (*a*) D. N. Woodruff, R. E. P. Winpenny and R. A. Layfield, *Chem. Rev.*, 2013, **113**, 5110–5148; (*b*) P. Zhang, Y.-N. Guo and J. Tang, *Coord. Chem. Rev.*, 2013, **257**, 1728–1763; (*c*) P. Zhang, L. Zhang and J. Tang, *Dalton Trans.*, 2015, **44**, 3923–3929.
26 S. T. Abtab, M. C. Majee, M. Maity, J. Titis, R. Boca and M. Chaudhury, *Inorg. Chem.*, 2014, **53**, 1295–1306.
27 A. Upadhyay, S. K. Singh, C. Das, R. Mondol, S. K. Langley, K. S. Murray, G. Rajaraman and M. Shanmugam, *Chem. Commun.*, 2014, **50**, 8838–8841.
28 G. Aromí and E. K. Brechin, *in Structure and Bonding*, Springer-Verlag, Berlin, 2006, pp. 1–67.
29 A. V. Funes, L. Carrella, E. Rentschler and P. Alborés, *Dalton Trans.*, 2014, **43**, 2361–2364.
30 S. K. Langley, N. F. Chilton, B. Moubaraki and K. S. Murray, *Inorg. Chem.*, 2013, **52**, 7183–7192.

31 S. K. Langley, L. Ungur, N. F. Chilton, B. Moubaraki, L. F. Chibotaru and K. S. Murray, *Inorg. Chem.*, 2014, **53**, 4303–4315.
32 S. K. Langley, N. F. Chilton, L. Ungur, B. Moubaraki, L. F. Chibotaru and K. S. Murray, *Inorg. Chem.*, 2012, **51**, 11873–11881.
33 S. K. Langley, D. P. Wielechowski, V. Vieru, N. F. Chilton, B. Moubaraki, L. F. Chibotaru and K. S. Murray, *Chem. Sci.*, 2014, **5**, 3246–3256.
34 P. S. Koroteev, N. N. Efimov, A. B. Ilyukhin, Z. V. Dobrokhotova and V. M. Novotortsev, *Inorg. Chim. Acta*, 2014, **418**, 157–162.
35 K. C. Mondal, G. E. Kostakis, Y. Lan, W. Wernsdorfer, C. E. Anson and A. K. Powell, *Inorg. Chem.*, 2011, **50**, 11604–11611.
36 K. C. Mondal, A. Sundt, Y. Lan, G. E. Kostakis, O. Waldmann, L. Ungur, L. F. Chibotaru, C. E. Anson and A. K. Powell, *Angew. Chem., Int. Ed.*, 2012, **51**, 7550–7554.
37 V. Mereacre, A. M. Ako, R. Clørac, W. Wernsdorfer, I. J. Hewitt, C. E. Anson and A. K. Powell, *Chem. – Eur. J.*, 2008, **14**, 3577–3584.
38 C. Papatriantafyllopoulou, W. Wernsdorfer, K. A. Abboud and G. Christou, *Inorg. Chem.*, 2011, **50**, 421–423.
39 L.-F. Zou, L. Zhao, Y.-N. Guo, G.-M. Yu, Y. Guo, J. Tang and Y.-H. Li, *Chem. Commun.*, 2011, **47**, 8659–8661.
40 V. Baskar, K. Gopal, M. A. Helliwell, F. Tuna, W. Wernsdorfer and R. E. P. Winpenny, *Dalton Trans.*, 2010, **39**, 4747–4750.
41 S. K. Langley, B. Moubaraki and K. S. Murray, *Dalton Trans.*, 2010, **39**, 5066–5069.
42 S. Takamatsu, T. Ishikawa, S. Koshihara and N. Ishikawa, *Inorg. Chem.*, 2007, **46**, 7250–7252.
43 F. Branzoli, P. Carretta, M. Filibian, G. Zoppellaro, M. J. Graf, J. R. Galan-Mascaros, O. Fuhr, S. Brink and M. Ruben, *J. Am. Chem. Soc.*, 2009, **131**, 4387–4396.
44 M. Gonidec, R. Biagi, V. Corradini, F. Moro, V. De Renzi, U. Pennino, D. Summa, L. Muccioli, C. Zannoni, D. B. Amabilino and J. Veciana, *J. Am. Chem. Soc.*, 2011, **133**, 6603–6612.
45 M. Hołyńska, D. Premužić, I.-R. Jeon, W. Wernsdorfer, R. Clérac and S. Dehnen, *Chem. – Eur. J.*, 2011, **17**, 9605–9610.
46 G. Rigaux, R. Inglis, S. Morrison, A. Prescimone, C. Cadiou, M. Evangelisti and E. K. Brechin, *Dalton Trans.*, 2011, **40**, 4797–4799.
47 J. Liu, W. Lin, Y. Chen, J. Leng, F. Guo and M. Tong, *Inorg. Chem.*, 2013, **52**, 457–463.
48 H. Chen, C.-B. Ma, M.-Q. Hu, H.-M. Wen and C.-N. Chen, *Dalton Trans.*, 2014, **43**, 16737–16744.
49 Q. Zhu, S. Xiang, T. Sheng, D. Yuan, C. Shen, C. Tan, S. Hu and X. Wu, *Chem. Commun.*, 2012, **48**, 10736–10738.
50 S. Ghosh, Y. Ida, T. Ishida and A. Ghosh, *Cryst. Growth Des.*, 2014, **14**, 2588–2598.
51 Z.-X. Wang, X. Zhang, Y.-Z. Zhang, M.-X. Li, H. Zhao, M. Andruh and K. R. Dunbar, *Angew. Chem., Int. Ed.*, 2014, **53**, 11567–11570.
52 F. J. Kettles, V. A. Milway, F. Tuna, R. Valiente, L. H. Thomas, W. Wernsdorfer, S. T. Ochsenbein and M. Murrie, *Inorg. Chem.*, 2014, **53**, 8970–8978.
53 H. L. C. Feltham, R. Clerac, L. Ungur, L. F. Chibotaru, A. K. Powell and S. Brooker, *Inorg. Chem.*, 2013, **52**, 3236–3240.
54 K.-Q. Hu, S.-Q. Wu, A.-L. Cui and H.-Z. Kou, *Transition Met. Chem.*, 2014, **39**, 713–718.
55 S. Xue, Y. Guo, L. Zhao, H. Zhang and J. Tang, *Inorg. Chem.*, 2014, **53**, 8165–8171.
56 J. Costes, F. Dahan and W. Wernsdorfer, *Inorg. Chem.*, 2006, **45**, 5–7.
57 L. Zhao, J. Wu, H. Ke and J. Tang, *Inorg. Chem.*, 2014, **53**, 3519–3525.
58 J. Sutter, S. Dhers, R. Rajamani, S. Ramasesha, J. P. Costes, C. Duhayon and L. Vendier, *Inorg. Chem.*, 2009, **48**, 5820–5828.
59 Y.-F. Zeng, G.-C. Xu, X. Hu, Z. Chen, X.-H. Bu, S. Gao and E. C. Sañudo, *Inorg. Chem.*, 2010, **49**, 9734–9736.
60 S.-J. Liu, Y.-F. Zeng, L. Xue, S.-D. Han, J.-M. Jia, T.-L. Hu and X.-H. Bu, *Inorg. Chem. Front.*, 2014, **1**, 200–206.
61 M. Li, Y. Lan, A. M. Ako, W. Wernsdorfer, C. E. Anson, G. Buth, A. K. Powell, Z. Wang and S. Gao, *Inorg. Chem.*, 2010, **49**, 11587–11594.
62 D. R. Turner, K. J. Berry, N. F. Chilton, B. Moubaraki, K. S. Murray, G. B. Deacon and S. R. Batten, *Dalton Trans.*, 2012, **41**, 11402–11412.
63 H. Chen, C. Ma, M. Hu, H. Wen, H. Cui, J.-Y. Liu, X.-W. Son and C.-N. Chen, *Dalton Trans.*, 2013, **42**, 4908–4914.
64 V. Chandrasekhar, B. M. Pandian, J. J. Vittal and R. Clerac, *Inorg. Chem.*, 2009, **48**, 1148–1157.
65 S. K. Langley, L. Ungur, N. F. Chilton, B. Moubaraki, L. F. Chibotaru and K. S. Murray, *Chem. – Eur. J.*, 2011, **17**, 9209–9218.
66 M. Murugesu, A. Mishra, W. Wernsdorfer, K. A. Abboud and G. Christou, *Polyhedron*, 2006, **25**, 613–625.
67 N. Ahmed, C. Das, S. Vaidya, S. K. Langley, K. S. Murray and M. Shanmugam, *Chem. – Eur. J.*, 2014, **20**, 14235–14239.
68 F. Gao, L. Cui, Y. Song, Y.-Z. Li and J.-L. Zuo, *Inorg. Chem.*, 2014, **53**, 562–567.
69 P. Bag, A. Chakraborty, G. Rogez and V. Chandrasekhar, *Inorg. Chem.*, 2014, **53**, 6524–6533.
70 J. Ruiz, G. Lorusso, M. Evangelisti, E. K. Brechin, S. J. A. Pope and E. Colacio, *Inorg. Chem.*, 2014, **53**, 3586–3594.
71 Y.-N. Guo, G.-F. Xu, Y. Guo and J. Tang, *Dalton Trans.*, 2011, **40**, 9953–9963.
72 L. Ungur, S.-Y. Lin, J. Tang and L. F. Chibotaru, *Chem. Soc. Rev.*, 2014, **43**, 6894–6905.
73 X. L. Li, F.-Y. Min, C. Wang, S.-Y. Lin, Z. Liu and J. Tang, *Dalton Trans.*, 2015, **44**, 3430–3438.
74 H. Ke, L. Zhao, Y. Guo and J. Tang, *Dalton Trans.*, 2012, **41**, 2314–2319.

